Note: High-speed Z tip scanner with screw cantilever holding mechanism for atomic-resolution atomic force microscopy in liquid

CrossMark
click for updates

Note: High-speed Z tip scanner with screw cantilever holding mechanism for atomic-resolution atomic force microscopy in liquid

Seyed Mohammad Reza Akrami,[1] Kazuki Miyata,[1] Hitoshi Asakawa,[2] and Takeshi Fukuma[1,3,a)]

[1]*Division of Electrical Engineering and Computer Science, Kanazawa University, Kakuma-machi, Kanazawa 920-1192, Japan*
[2]*Bio-AFM Frontier Research Center, Kanazawa University, Kakuma-machi, Kanazawa 920-1192, Japan*
[3]*ACT-C, Japan Science and Technology Agency, Honcho 4-1-9, Kawaguchi 332-0012, Japan*

High-speed atomic force microscopy has attracted much attention due to its unique capability of visualizing nanoscale dynamic processes at a solid/liquid interface. However, its usability and resolution have yet to be improved. As one of the solutions for this issue, here we present a design of a high-speed Z-tip scanner with screw holding mechanism. We perform detailed comparison between designs with different actuator size and screw arrangement by finite element analysis. Based on the design giving the best performance, we have developed a Z tip scanner and measured its performance. The measured frequency response of the scanner shows a flat response up to $\sim$10 kHz. This high frequency response allows us to achieve wideband tip-sample distance regulation. We demonstrate the applicability of the scanner to high-speed atomic-resolution imaging by visualizing atomic-scale calcite crystal dissolution process in water at 2 s/frame. © *2014 AIP Publishing LLC*. [http://dx.doi.org/10.1063/1.4904029]

There have been strong demands for nanoscale visualization techniques in various research fields such as biology, chemistry, physics, and industry. Atomic force microscopy (AFM)[1] has been a powerful tool for such nanoscale visualization. AFM can be operated not only in liquid but also in air and vacuum. It can be used for imaging insulating materials as well as conductive ones. Owing to these unique capabilities, AFM has been used in wide range of applications.

High-speed operation of AFM has been demanded for imaging dynamic processes at solid/liquid interfaces. The enhancement of AFM operation speed requires improvement of all the mechanical and electrical components constituting the tip-sample distance regulation feedback loop. Among them, a scanner is one of the most important components that strongly influence the operation speed and usability of AFM. Therefore, efforts have been made for enhancing the resonance frequency of a scanner and reducing the cross talk between XY and Z scanners.[2–10] These previous developments are well summarized in review articles.[11,12] Owing to these previous works, high-speed AFM has been developed[2,3,13] and used for visualizing various processes such as crystal growth[13,14] and biological phenomena.[15,16]

In contrast, applications of high-speed AFM to atomic-scale studies on interfacial phenomena have been very limited.[17,18] Atomic-resolution imaging imposes stringent requirements on the design of a high-speed scanner and a high-voltage amplifier (HVAMP) used for driving the scanner. In our previous study,[17] we presented a design of separate-type high-speed scanner that consists of XY sample and Z tip scanners. In addition, we presented the design of a wideband and

a low noise HVAMP to achieve sufficient noise performance to allow high-speed and high-resolution imaging.

In the previous work,[17] we compared different cantilever holding mechanisms using a screw, a plate spring, and glue. The result showed that the screw holding mechanism gives the best balance between the performance and the usability. However, the design variations of the Z tip scanner with a screw holding mechanism were not considered to improve the performance. For example, the dependence of the performance on actuator size and screw arrangement has not been investigated.

In this study, we investigate the performance of Z tip scanners with different designs of a cantilever screw holding mechanism. We investigate the dependence of the frequency response and vibration modes of the scanner on the design by finite element analysis (FEA). Based on the design giving the best performance, we develop a scanner and experimentally measure the performance. Finally, we demonstrate applicability of the developed scanner to atomic-resolution imaging by imaging calcite crystal dissolution process at 2 s/frame in water.

FEA software (COMSOL Multiphysics, COMSOL) was used for theoretical analysis of the frequency response and vibration modes of the scanner. We used Young's Modulus of 193 GPa, Poisson's ratio of 0.25 and density of 7970 kg/m^3 for modeling the scanner bodies made of SS316. For modeling the stack piezoactuators, we used density of 7500 kg/m^3. Coupling and elasticity matrices of them were determined by measuring the displacement and resonance frequency of a piezoactuator fixed to a large body. We measured frequency response of the developed scanner by frequency response analyzer (FRA5097, NF). We measured displacement of the Z scanner by detecting the vibration of cantilever body attached

---

(a) Design I with 2×2 actuator

(b) Design I with 3×3 actuator

(c) Design II with 2×2 actuator

(d) Design II with 3×3 actuator

FIG. 1. Schematic models of the *Z* tip scanners with different designs of a cantilever screw holding mechanism.

FIG. 2. Frequency responses of the *Z* scanners with different cantilever holding mechanisms obtained by FEA.

to the cantilever stage using a heterodyne laser displacement sensor (ST-3761, IWATSU).

For AFM imaging, we used a home-built AFM system with an ultralow noise cantilever deflection sensor.[19–21] We performed phase modulation AFM (PM-AFM) imaging of a cleaved surface of a calcite crystal (Furuuchi Chemical) using a cantilever with a spring constant of ∼85 N/m (AC55, Olympus). We used the *XY* sample scanner and the HVAMP that we previously developed.[18] All the AFM experiments were performed at room temperature in water.

Figure 1 shows schematic models of the *Z* tip scanners with different cantilever screw holding mechanisms. These designs are different in actuator size and screw arrangement. The screw is laterally displaced from the cantilever position in Figs. 1(a) and 1(b) while vertically displaced in Figs. 1(c) and 1(d). Here we refer to the former as Design I and the latter as Design II. The actuator in Figs. 1(a) and 1(c) has a smaller size ($2 \times 2 \times 2$ mm^3) while the one in Figs. 1(b) and 1(d) has a larger size ($3 \times 3 \times 2$ mm^3). An actuator is fixed to a holder body with glue. Then, a cantilever stage is fixed on the actuator. A cantilever is sandwiched between the cantilever stage and a metal plate spring. The plate spring is fixed with a screw to the cantilever stage. All the metal parts are made of stainless steel (SS316). The design I with a 3×3 actuator is the same design as we previously reported in Ref. 17.

In Design II, we found that the design of the plate spring is important. If we use a plate spring manufactured by bending a metal plate with a uniform thickness, it is easily fatigued by repeated use. In addition, the holding force is insufficient so that spurious resonances appear in the low frequency range. We found that this problem can be solved by using a precisely machined metal plate with a variable thickness. This design gives a sufficient holding force and allows repeated exchange of cantilevers.

Figure 2 shows frequency response of the *Z* scanners with different cantilever holding mechanisms calculated by FEA. These curves show several peaks corresponding to the vibration modes of the scanners. Figure 3 shows the first four vibration modes (Modes 1–4) of the *Z* scanners calculated by FEA.
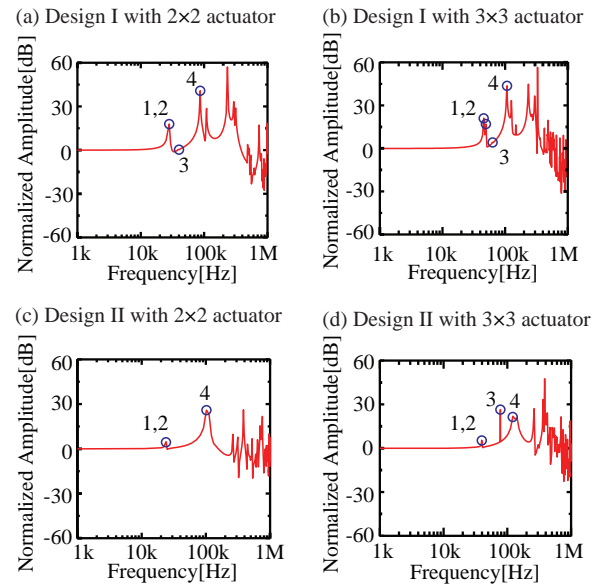
These vibration modes correspond to the peaks indicated by the circles in Fig. 2.

For all the designs, the lowest frequency peak (Mode 1) corresponds to the swinging motion of the actuator and the cantilever stage. Thus, the frequency of this vibration mode should determine the maximum frequency for driving the scanner. The results show that the frequency of Mode 1 obtained with the larger actuator (Figs. 1(b) and 1(d)) is higher than that with the smaller actuator (Figs. 1(a) and 1(c)).

Due to the small width of the smaller actuator, the aspect ratio of the structure consisting of the actuator and the cantilever stage is relatively high. This should account for the
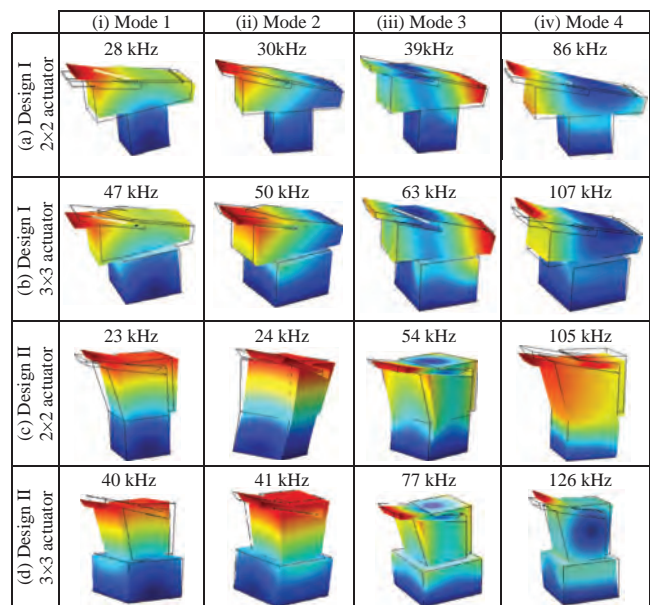

FIG. 3. Vibration modes of the *Z* tip scanners with different cantilever holding mechanisms obtained by FEA.
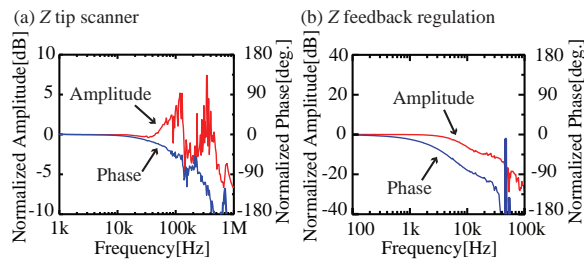
FIG. 4. Frequency response of (a) the developed Z tip scanner and (b) Z feedback regulation measured in contact-mode AFM.
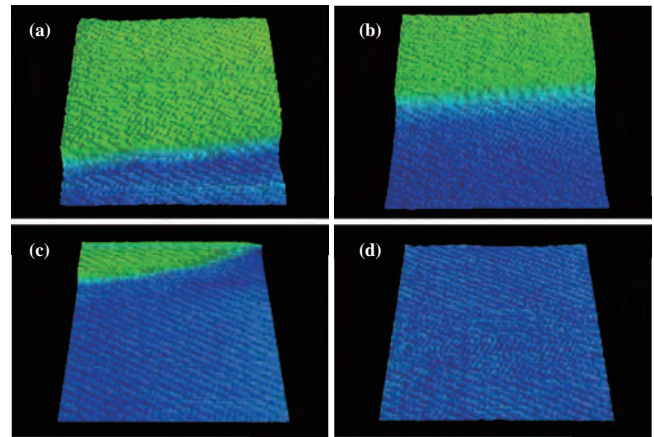

FIG. 5. Snapshots of successive PM-AFM images of calcite crystal dissolution process in water: (a) 0 s, (b) 20 s, (c) 32 s, and (d) 40 s. Scan size: 20 × 20 nm^2. Scan rate: 250 Hz. Imaging speed: 2 s/frame. Pixel size: 500 × 500 pix^2. Tip velocity: 10 μm/s.

lower resonance frequency observed for the scanner with the smaller actuator.

The lowest frequency peaks of the curves in Figs. 2(b) and 2(d) are found at 47 kHz and 40 kHz, respectively. Although the result suggests that Design I provides slightly higher resonance frequency, the difference is not significant. In contrast, the magnitude of the peak is significantly different between these two designs. The peak height in the curve obtained by Design II is much lower than that in the curve obtained by Design I. This is practically useful as it allows a better compensation by the Q-control method for further improvement of the frequency response.[11] In Design I, the cantilever stage is laterally protruded from the side of the actuator. This should enhance the magnitude of the swinging vibration. These results suggest that Design II with a 3 × 3 actuator should give the best performance among these designs.

Based on the analysis presented above, we have developed a Z tip scanner with Design II and a 3 × 3 actuator. Figure 4(a) shows frequency response of the developed Z tip scanner. The amplitude curve shows a broad peak from 40 kHz to 130 kHz. This frequency range agrees with the frequencies of Modes 1–4 shown in Fig. 2(d) although they are not separately observed.

Figure 4(b) shows frequency response of the tip-sample distance regulation measured by contact-mode AFM. The feedback gains are adjusted such that the bandwidth is maximized. The amplitude curve shows that −3 dB bandwidth of the feedback regulation is ∼6 kHz. This is sufficient for performing high-speed AFM imaging at a few seconds per frame as demonstrated below.

Figure 5 shows snapshots of successive PM-AFM images of calcite crystal dissolution process. In spite of the fast scanning speed (2 s/frame), the images show atomic-scale contrasts with a periodicity of ∼0.5 nm. The images also show that the movement of a step edge from the top to the bottom of the image. The atomically sharp step edge is visualized in the images, which demonstrates the true atomic resolution of the PM-AFM imaging. The result demonstrates that the developed scanner is applicable to atomic-scale high-speed AFM imaging in liquid.

In this study, we have compared the performance of high-speed Z tip scanners with a screw cantilever holding mechanism by FEA. Based on the results, we have developed a scanner with the improved actuator size and screw arrangement. In addition, we have demonstrated that the developed scanner is applicable to high-speed atomic-resolution imaging in liquid by visualizing calcite crystal dissolution process in real time. This work has improved the understanding on the design of high-speed atomic-resolution AFM for liquid-environment applications.

[1] G. Binnig, C. F. Quate, and Ch. Gerber, Phys. Rev. Lett. **56**, 930 (1986).
[2] T. Ando, N. Kodera, E. Takai, D. Maruyama, K. Saito, and A. Toda, Proc. Natl. Acad. Sci. U.S.A. **98**, 12468 (2001).
[3] A. D. L. Humphris, M. J. Miles, and J. K. Hobbs, Appl. Phys. Lett. **86**, 034106 (2005).
[4] J. H. Kindt, G. E. Fantner, J. A. Cutroni, and P. K. Hansma, Ultramicroscopy **100**, 259 (2004).
[5] G. E. Fantner, G. Schitter, J. H. Kindt, T. Ivanov, K. Ivanova, R. Patel, N. Holten-Andresen, J. Adams, P. J. Thurner, I. W. Rangelow, and P. K. Hansma, Ultramicroscopy **106**, 881 (2006).
[6] G. Schitter, P. J. Thurner, and P. K. Hansma, Mechatronics **18**, 282 (2008).
[7] I. S. Bozchalooi, K. Youcef-Toumi, D. J. Burns, and G. E. Fantner, Rev. Sci. Instrum. **82**, 113712 (2011).
[8] C. Braunsmann and T. E. Schäffer, Nanotechnology **21**, 225705 (2010).
[9] F. C. Tabak, E. C. M. Disseldorp, G. H. Wortel, A. J. Katan, M. B. S. Hesselberth, T. H. Oosterkamp, J. W. M. Frenken, and W. M. van Spengen, Ultramicroscopy **110**, 599 (2010).
[10] T. Fukuma, H. Okazaki, N. Kodera, T. Uchihashi, and T. Ando, Appl. Phys. Lett. **92**, 243119 (2008).
[11] T. Ando, T. Uchihashi, and T. Fukuma, Prog. Surf. Sci. **83**, 337, (2008).
[12] Y. K. Yong, S. O. R. Moheimani, B. J. Kenton, and K. K. Leang, Rev. Sci. Instrum. **83**, 121101 (2012).
[13] G. T. Paloczi, B. L. Smith, P. K. Hansma, D. A. Walters, and M. A. Wendman, Appl. Phys. Lett. **73**, 1658 (1998).
[14] J. K. Hobbs, C. Vasilev, and A. D. L. Humphris, Polymer **46**, 10226 (2005).
[15] N. Kodera, D. Yamamoto, R. Ishikawa, and T. Ando, Nature (London) **468**, 72 (2010).
[16] T. Uchihashi, R. Iino, T. Ando, and H. Noji, Science **333**, 755 (2011).
[17] K. Miyata, S. Usho, S. Yamada, S. Furuya, K. Yoshida, H. Asakawa, and T. Fukuma, Rev. Sci. Instrum. **84**, 043705 (2013).
[18] K. Miyata, H. Asakawa, and T. Fukuma, Appl. Phys. Lett. **103**, 203104 (2013).
[19] T. Fukuma, M. Kimura, K. Kobayashi, K. Matsushige, and H. Yamada, Rev. Sci. Instrum. **76**, 053704 (2005).
[20] T. Fukuma and S. P. Jarvis, Rev. Sci. Instrum. **77**, 043701 (2006).
[21] T. Fukuma, Rev. Sci. Instrum. **80**, 023707 (2009).